In conclusion, we have developed a novel procedure for the demetalation of tricarbonyl(η^4-cyclopentadienone)iron complexes, which proceeds by a ligand exchange initiated by sodium hydroxide. The X-ray analysis of an intermediate dimeric complex revealed an extraordinary nearly square-planar coordinated sodium ion.

Experimental Section

General procedure for the demetalation of the bicyclic tricarbonyl(η^4-cyclopentadienone)iron complexes **1** by NaOH-initiated ligand exchange: A solution of complex **1** (0.478 mmol) in THF (8 mL) and aqueous 1M NaOH (4 mL) was stirred for 2.5 h under an argon atmosphere. Then 1-iodopentane was added (0.15 mL, 228 mg, 1.15 mmol) and the yellow solution turned brown. After stirring the mixture for an additional 15 min under argon, H_3PO_4 (0.15 mL) was added, the organic layer was separated, and the aqueous layer was extracted with diethyl ether. The combined organic layers were dried over Na_2SO_4 and filtered through a short path of silica gel. After addition of $Na_2S_2O_3$ (200 mg) and Celite (200 mg) the filtrate was stirred slowly in the air for 3 h in the presence of daylight. Filtration through a short path of Celite, evaporation of the solvent, and flash chromatography (pentane/diethyl ether) of the residue on silica gel provided the free ligand **6**.

Received: February 9, 1999 [Z13016IE]
German version: *Angew. Chem.* **1999**, *111*, 2196 – 2199

Keywords: cyclopentadienones · hydrido complexes · iron · sodium · synthetic methods

[1] a) H.-J. Knölker, J. Heber, C. H. Mahler, *Synlett* **1992**, 1002; b) H.-J. Knölker, J. Heber, *Synlett* **1993**, 924; c) H.-J. Knölker, E. Baum, J. Heber, *Tetrahedron Lett.* **1995**, *36*, 7647.

[2] a) A. J. Pearson, R. J. Shively, R. A. Dubbert, *Organometallics* **1992**, *11*, 4096; b) A. J. Pearson, R. J. Shively, *Organometallics* **1994**, *13*, 578; c) A. J. Pearson, X. Yao, *Synlett* **1997**, 1281.

[3] Y. Shvo, E. Hazum, *J. Chem. Soc. Chem. Commun.* **1974**, 336; H.-J. Knölker, *J. Prakt. Chem.* **1996**, *338*, 190.

[4] H.-J. Knölker, H. Goesmann, R. Klauss, *Angew. Chem.* **1999**, *111*, 727; *Angew. Chem. Int. Ed.* **1999**, *38*, 702.

[5] a) W. Hieber, F. Leutert, *Z. Anorg. Allg. Chem.* **1932**, *204*, 145; b) W. Reppe, H. Vetter, *Liebigs Ann. Chem.* **1953**, *582*, 133.

[6] R. J. Kazlauskas, M. S. Wrighton, *Organometallics* **1982**, *1*, 602.

[7] Spectroscopic data: **2a**: IR (KBr): $\tilde{\nu}$ = 3581, 1991, 1932 cm^{-1}; ^{1}H NMR (400 MHz, C_6D_6): δ = −11.62 (s, 1H), 0.30 (s, 18H), 1.23 (m, 2H), 1.45 (m, 2H), 2.01 (m, 2H), 2.36 (m, 2H), 3.75 (s, 1H); ^{13}C NMR and DEPT (100 MHz, C_6D_6): δ = 1.48 (6CH_3), 23.65 (2CH_2), 26.09 (2CH_2), 70.73 (2C), 103.61 (2C), 146.18 (C), 217.57 (CO), 217.64 (CO); elemental analysis calcd for $C_{17}H_{28}FeO_3Si_2$: C 52.03, H 7.19; found: C 51.97, H 7.21. **3a**: IR (KBr): $\tilde{\nu}$ = 3584, 2011, 1968 cm^{-1}; ^{1}H NMR (400 MHz, C_6D_6): δ = 0.35 (s, 18H), 1.03 (m, 2H), 1.13 (m, 2H), 1.87 (m, 2H), 2.14 (m, 2H), 4.34 (s, 1H); ^{13}C NMR and DEPT (125 MHz, C_6D_6): δ = 1.34 (6CH_3), 22.81 (2CH_2), 24.92 (2CH_2), 75.65 (2C), 102.15 (2C), 147.74 (C), 216.57 (2CO); elemental analysis calcd for $C_{17}H_{27}FeIO_3Si_2$: C 39.39, H 5.25; found: C 39.54, H 5.10. **4a**: IR (KBr): $\tilde{\nu}$ = 2000, 1967, 1943, 1859, 1836, 1819 cm^{-1}; IR (CH_3OH): $\tilde{\nu}$ = 1997, 1970, 1937, 1904 cm^{-1}; ^{1}H NMR (500 MHz, CD_3OD): δ = −13.05 (s, 1H), 0.25 (s, 18H), 1.56 (m, 2H), 1.72 (m, 2H), 2.30 (m, 2H), 2.52 (m, 2H); ^{13}C NMR and DEPT (125 MHz, CD_3OD): δ = 1.56 (6CH_3), 24.60 (2CH_2), 27.49 (2CH_2), 68.47 (2C), 102.53 (2C), 170.13 (C=O), 221.06 (CO), 221.18 (CO). **5a**: IR (KBr): $\tilde{\nu}$ = 1993, 1957, 1911, 1492 cm^{-1}; IR (CH_3OH): $\tilde{\nu}$ = 1992, 1937 cm^{-1}; ^{13}C NMR and DEPT (125 MHz, CD_3OD): δ = 1.11 (6CH_3), 23.93 (2CH_2), 26.67 (2CH_2), 65.41 (2C), 106.29 (2C), 176.05 (C=O), 219.17 (2CO); elemental analysis calcd for $C_{21}H_{34}FeINaO_4Si_2$: C 41.19, H 5.60; found: C 41.14, H 5.52.

[8] X-ray crystal structure analyses: **2a**: yellow needles, $C_{17}H_{28}FeO_3Si_2$; M_r = 392.42 g mol^{-1}, triclinic, space group $P\bar{1}$, λ = 0.71073 Å, a = 6.7797(4), b = 11.2561(8), c = 13.9334(12) Å, α = 104.343(5), β = 92.265(5), γ = 97.624(4)°, V = 1018.14(13) Å^3, Z = 2, μ = 0.868 mm^{-1}, ρ_{calcd} = 1.280 g cm^{-3}, T = 200(2) K, θ range: 2.70 – 27.50°; 4598 independent reflections; full-matrix least squares on F^2; R_1 = 0.0272, wR_2 = 0.0710 [$I > 2\sigma(I)$]; maximal residual electron density 0.620 e Å^{-3}. All hydrogen atoms were determined by Fourier difference calculation and refined isotropically. **5a**: brown cubes, $C_{17}H_{26}FeINaO_3Si_2 \cdot C_4H_8O$; M_r = 612.40 g mol^{-1}, monoclinic, space group $P2_1/n$, λ = 0.71073 Å, a = 11.254(2), b = 15.508(3), c = 15.254(3) Å, β = 93.52(3)°, V = 2657.2(9) Å^3, Z = 4, ρ_{calcd} = 1.531 g cm^{-3}, μ = 1.859 mm^{-1}, T = 200(2) K, θ range: 1.87 – 25.50°; 4950 independent reflections; full-matrix least squares on F^2; R_1 = 0.0390, wR_2 = 0.0712 [$I > 2\sigma(I)$]; maximal residual electron density 0.565 e Å^{-3}. Programs: G. M. Sheldrick, SHELXS-86 (Göttingen, **1986**), SHELXL-93 (Göttingen, **1993**); E. Keller, SCHAKAL-97 (Freiburg im Breisgau, **1997**). Crystallographic data (excluding structure factors) for the structures reported in this paper have been deposited with the Cambridge Crystallographic Data Centre as supplementary publication no. CCDC-114303 (**5a**) and CCDC-114304 (**2a**). Copies of the data can be obtained free of charge on application to CCDC, 12 Union Road, Cambridge CB2 1EZ, UK (fax: (+44) 1223-336-033; e-mail: deposit@ccdc.cam.ac.uk).

[9] Compare: a) E. Weiss, W. Hübel, R. Merényi, *Chem. Ber.* **1962**, *95*, 1155; b) E. Weiss, R. Merényi, W. Hübel, *Chem. Ber.* **1962**, *95*, 1170.

[10] For distorted tetrahedral or square-pyramidal coordinations at sodium centers, see for example S. G. Bott, A. W. Coleman, J. L. Atwood, *J. Am. Chem. Soc.* **1986**, *108*, 1709; M. Veith, J. Böhnlein, V. Huch, *Chem. Ber.* **1989**, *122*, 841; M. Hong, F. Jiang, X. Huang, W. Su, W. Li, R. Cao, H. Liu, *Inorg. Chim. Acta* **1997**, *256*, 137; E. Gallo, E. Solari, N. Re, C. Floriani, A. Chiesi-Villa, C. Rizzoli, *J. Am. Chem. Soc.* **1997**, *119*, 5144.

[11] a) N. A. Bailey, R. Mason, *Acta Crystallogr.* **1966**, *21*, 652; b) K. Hoffmann, E. Weiss, *J. Organomet. Chem.* **1977**, *128*, 237; c) G. G. Cash, R. C. Pettersen, *Inorg. Chem.* **1978**, *17*, 650; d) D. Fornals, M. A. Pericàs, F. Serratosa, J. Vinaixa, M. Font-Altaba, X. Solans, *J. Chem. Soc. Perkin Trans. 1* **1987**, 2749.

[12] D. G. Alway, K. W. Barnett, *Inorg. Chem.* **1978**, *17*, 2826; X. Pan, C. E. Philbin, M. P. Castellani, D. R. Tyler, *Inorg. Chem.* **1988**, *27*, 671.

A Molybdenum – Iron – Sulfur Cluster Containing Structural Elements Relevant to the P-Cluster of Nitrogenase**

Frank Osterloh, Yiannis Sanakis, Richard J. Staples, Eckard Münck,* and Richard H. Holm*

The commonly occurring iron – sulfur cluster cores—rhomboidal Fe_2S_2, cuboidal Fe_3S_4, and cubane-type Fe_4S_4—have been synthesized in research directed toward an understand-

[*] Prof. Dr. E. Münck, Dr. Y. Sanakis
Department of Chemistry
Carnegie Mellon University
Pittsburgh, PA 15213 (USA)
Fax: (+1) 412-268-1061
E-mail: em40@andrew.cmu.edu
Prof. Dr. R. H. Holm, Dr. F. Osterloh, Dr. R. J. Staples
Department of Chemistry and Chemical Biology
Harvard University
Cambridge, MA 02138 (USA)
Fax: (+1) 617-496-9289
E-mail: holm@chemistry.harvard.edu

[**] This work was supported by grants from the National Institutes of Health (GM 28856 at Harvard University) and the National Science Foundation (MCB 94-06224 at Carnegie Mellon University). F.O. thanks the Deutsche Forschungsgemeinschaft (DFG) for a postdoctoral fellowship.

ing of the formation, structure, and function of these clusters in biology.[1] Our current endeavors are directed toward the synthesis of more complicated metal site structures, described as bridged cluster assemblies[2] and including the two cluster types in the MoFe protein of nitrogenase.[3] The P-cluster **1** contains an Fe_8S_7 core formed by two cuboidal Fe_4S_3 fragments bridged by a central sulfur atom, with additional bridging by two cysteinyl sulfur atoms.[4] The FeMo cofactor

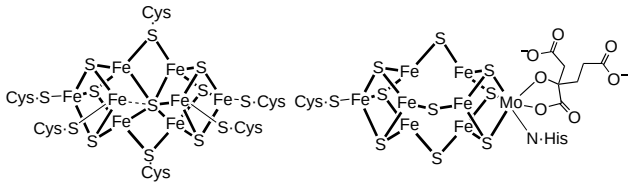

1 (P^N state) **2**

(FeMoco) cluster **2** has an $MoFe_7S_9$ core with cuboidal Fe_4S_3 and $MoFe_3S_4$ clusters bridged by three μ_2-S atoms. The P-cluster appears to mediate electron transfer from the Fe protein to FeMoco, which is the catalytic site.[5]

Recently, we reported a compositional analogue of FeMoco in the form of the sulfido-bridged double cubane core $[Fe_4S_4$-S-$MoFe_3S_4]$.[6] The symmetrical double cubane $[MoFe_3S_4$-S-$MoFe_3S_4]$ has also been prepared. In these species, the individual clusters are bridged by μ_2-sulfide units and are in their oxidized states ($[Fe_4S_4]^{2+}$, $[MoFe_3S_4]^{3+}$). The iron populations of as-isolated FeMoco ($S = 3/2$) and P-cluster (P^N state) are substantially reduced. For the cofactor, the ^{57}Fe isomer shift of $\delta = 0.47\ mm\,s^{-1}$ at 4.2 K[7] is not inconsistent with trigonal $Fe^{II}S_3$ coordination,[8] and a recent ^{57}Fe ENDOR analysis leads to the valence description $Mo^{IV} + Fe^{III} + 6\,Fe^{II}$.[9] The isomer shifts of the P-cluster ($\delta \approx 0.64\ mm\,s^{-1}$ at 4.2 K) are consistent with an all-Fe^{II} P^N state.[10] Consequently, we have initiated a second synthetic approach to FeMoco and P-cluster utilizing as precursors cubane-type clusters in more reduced states.

The rhomb-bridged double cubane $[(Cl_4cat)_2Mo_2Fe_6S_8(PEt)_6]$[11] (**3**) is one of several species whose reduced cores ($[Fe_4S_4]^{1+}$, $[MoFe_3S_4]^{2+}$) are stabilized in isolable compounds by phosphane ligation.[12] A suspension of **3** in acetonitrile was treated with two equivalents of $(Et_4N)(SH)$ to give a dark solution (Scheme 1). Evaporation of solvent to remove PEt_3

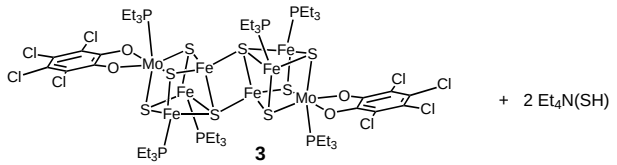

Scheme 1. Preparation of $(Bu_4N)_2(Et_4N)_6$[**4**]. 1. Stirring in CH_3CN at room temperature for 12 h followed by evaporation of all volatile components (CH_3CN, PEt_3, H_2S) in vacuo. 2. Extraction of the solid residue with NMF, addition of solid $(Bu_4N)(PF_6)$, and crystallization from NMF/diethyl ether.

and H_2S followed by extraction of the solid residue with *N*-methylformamide (NMF) afforded a black solution, whose major component could be crystallized after addition of $(Bu_4N)(PF_6)$. Vapor diffusion of diethyl ether into the solution for three days caused separation of black crystals of $(Bu_4N)_2(Et_4N)_6[(Cl_4cat)_6(Et_3P)_6Mo_6Fe_{20}S_{30}] \cdot 9\,NMF$ in 33 % yield. This compound contains cluster **4** and was identified crystallographically; the NMF molecules are uncoordinated. This is the highest nuclearity Fe–S or heterometallic Fe–S cluster currently known. Certain of its fragments are of interest in relation to the P-cluster of nitrogenase.

Two perspectives of the $[Mo_6Fe_{20}S_{30}]^{8-}$ core of **4** are presented in Figure 1, from which it is evident that the structure is centrosymmetric with idealized C_{2h} symmetry. The

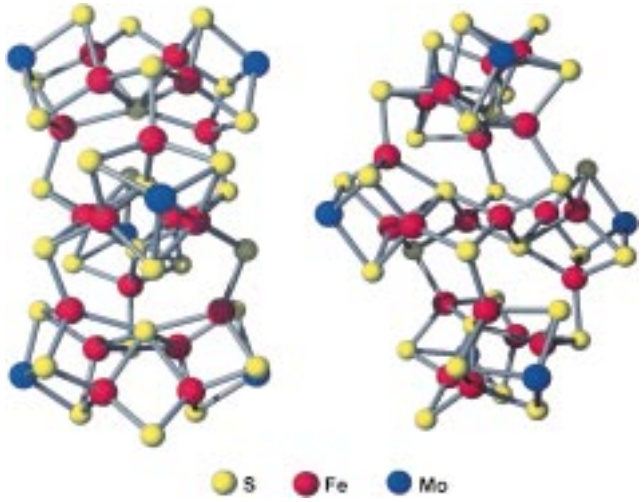

Figure 1. Front (left) and side views (right) of the $Mo_6Fe_{20}S_{30}$ core of cluster **4**, which has crystallographic inversion symmetry and idealized C_{2h} symmetry. The upper and lower $Mo_2Fe_6S_9$ fragments (Figure 2) are connected to the central $Mo_2Fe_8S_{12}$ fragment (Figure 3) by six μ_3-Fe-S bridges. Terminal ligands on the molybdenum atoms are omitted for clarity. Selected mean bond lengths [Å] for the distorted octahedral Mo(Cl_4cat)-(PEt_3)S_3 coordination unit: Mo–O 2.126(8), Mo–P 2.63(3), Mo–S 2.37(3).

initial double cubane structure of precursor **3** has undergone fracture and rearrangement, resulting in removal of terminal ligands at the iron sites; in this sense, **4** resembles the cyclic cluster $[Na_2Fe_{18}S_{30}]^{8-}$.[13] The sulfur atoms divide into the bridging modes $2 \times \mu_2 + 24 \times \mu_3 + 2 \times \mu_5 + 2 \times \mu_6$. The structure can be described in terms of three fragments: The upper and lower fragments $Mo_2Fe_6S_9$ are symmetry-related and have the structure shown in Figure 2. The central fragment $Mo_2Fe_8S_{14}$ (see Figure 3) is connected to the upper and lower fragments by six μ_3-S–Fe bridges (2.230(4) – 2.273(5) Å) involving S(8,14,15) and their symmetry-related counterparts. Within both types of fragments, the Fe–S distances increase in the order Fe–μ_2-S < Fe–μ_3-S < Fe–μ_5-S $\lesssim$ Fe–μ_6-S.

The $Mo_2Fe_6S_9$ fragment (Figure 2) has idealized C_s symmetry and contains two $MoFe_3S_4$ cubane units, as does **3**. However, one sulfur atom is common to both, resulting in an S(9)Fe_6(1 – 6) grouping and a μ_6 bridging function for S(9). Atoms Fe(2,5) and Fe(1,4) are additionally bridged by μ_2-S(7) and μ_3-S(8). Consequently, S(9) is shared by eight nonplanar rhomb-like Fe_2S_2 units, an opposite pair of which

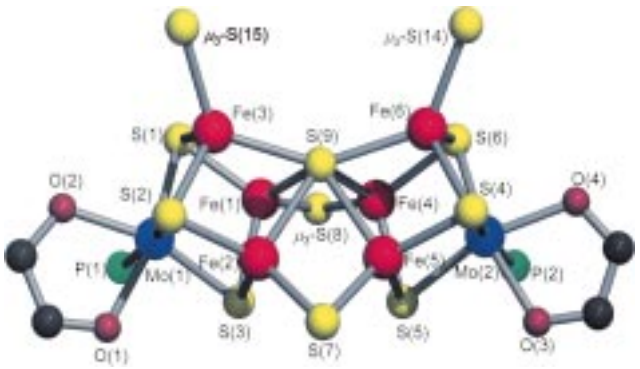

Figure 2. Structure of the upper and lower $Mo_2Fe_6S_9$ fragment of cluster **4** with idealized C_s symmetry. Atom μ_3-S(8) bridges to Fe(7a) of the central fragment and atoms μ_3-S(14,15), which bridge to Fe(3,6), are part of that fragment (Figure 3); atom S(7) is bound to two Fe atoms in a μ_2 manner. At Mo(1,2), the catecholate chelate rings and coordinated P atoms of PEt_3 ligands are indicated. Selected (mean) bond lengths [Å] and angles [°]: Mo–Fe 2.74(1), intracubane Fe–Fe 2.74(2), Fe(1)–Fe(4) 2.635(3), Fe(2)–Fe(5) 2.681(3), Fe–S(9) 2.40(2), Fe(1,2,4,5)–S(9) 2.39(1), Fe–S(1–6) 2.24(2), Fe(2,5)–S(7) 2.190(8); Fe(3)-S(9)-Fe(6) 145.3(2), Fe(2)-S(7)-Fe(5) 75.5(1), Fe(1)-S(8)-Fe(4) 71.9(1), Fe-S(9)-Fe 69.0(6). Atoms (*n*) and (*n*a) are related by symmetry.

(Fe_2(1,2)S_2(3,9) and Fe_2(4,5)S_2(5,9)) are faces of the $MoFe_3S_4$ cubanes. The S(7,8) bridging interactions force a large Fe(3)-S(9)-Fe(6) angle of 145.3(2)°. Intracubane bond angles at S(9) occur in the range of 68.9–70.4°. The intracubane mean Mo–Fe (2.74(1) Å) and Fe–Fe distances (2.74(2) Å) are both substantially longer than the corresponding mean values in **3** (2.677(5) and 2.639(2) Å,[11] respectively). However, intracubane Fe–S distances are unchanged (2.24(2) Å). The μ_6-S bridging mode is precedented—in $[Ni_9S(StBu)_8]^{1-}$[14] the core topology resembles that of **2**—but is otherwise unknown in Fe–S clusters.

The most striking feature of the $Mo_2Fe_6S_9$ fragment is its structural resemblance to the $Fe_8S_7(SR)_2$ portion of the P-cluster **1**, whose composition can be derived by replacing $Mo(Cl_4cat)(PEt_3)$ with $Fe^{II}(SR)$ and S(7,8,14,15) with RS^-. The topologies of the fragment and **1** are clearly similar but with some structural differences. In the P^N state, the central sulfur atom exhibits unsymmetrical 5 + 1 coordination with one long Fe–S bond of 2.9 Å,[4] and is best considered as μ_5-S. In the fragment, the six Fe–S(9) distances are in the range of 2.381(4)–2.429(5) Å with a mean of 2.40(2) Å; the sulfur atom is clearly μ_6-S. Otherwise, the adjacent Fe–Fe separations in the P^N state obtained from X-ray (2.4–2.8 Å)[4] and EXAFS analyses[15] (mean values 2.57, 2.75 Å) cover the range observed for the fragment (2.635(3)–2.771(3) Å).

Certain distortions not found elsewhere in the $Mo_2Fe_6S_9$ fragment occur at Fe(1,4/2,5), which are bound to μ_2-S(7)/μ_3-S(8). The FeS_4 units are distorted toward trigonal-pyramidal coordination with S(9) as the axial ligand. At these sites, differences between axial and mean equatorial bond lengths are 0.16–0.17 Å, axial bond angles average to 105(1)°, and the range of equatorial bond angles is 103–124°. Distortions of this type occur in $FePS_3$ sites of Mo/V-Fe-S clusters.[16] Limiting elongated distortion generates trigonal-planar coordination, similar to that observed for six iron sites in **2**. Note that the structures of **1** and **2** are formally interconvertible. Movement of the μ_5-S atom out of the center of the Fe_6 trigonal prism with attendant cleavage of four Fe–S bonds and transformation of tetrahedral FeS_4 into trigonal FeS_3 sites recovers the topology of the cofactor core. Signs of this transformation are integrated into the structure of the $Mo_2Fe_6S_9$ fragment, whose structure could be interpreted as transitional between P-cluster and FeMoco topology.

The structure of the central $Mo_2Fe_8S_{12}$ fragment of cluster **4** is presented in Figure 3. Metric parameters of the molybdenum coordination unit and analogous Fe–μ-S interactions are

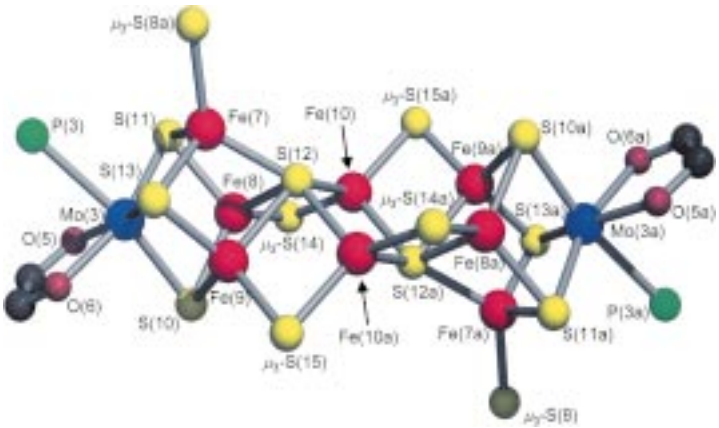

Figure 3. Structure of the central $Mo_2Fe_8S_{12}$ fragment of cluster **4** with a crystallographic inversion center and idealized C_{2h} symmetry. Atoms μ_3-S(8,8a) are parts of two $Mo_2Fe_6S_9$ fragments, and atoms μ_3-S(14/14a) and μ_3-S(15/15a) bridge to Fe(6/6a) and Fe(3/3a), respectively, of those fragments. Selected (mean) bond lengths [Å] and angles [°]: Fe(7)–S(12) 2.292(4), Fe(8–10)–S(12) 2.346(2), Fe(10)–S(15a) 2.275(4), Fe(10)–Fe(10a) 3.462(3); Fe(7)-S(12)-Fe(10) 132.5(2), S(12)-Fe(10)-S(12a) 85.0(2), Fe(10)-S(12)-Fe(10a) 95.0(2), S(14)-Fe(10)-S(12a) 126.9(2), S(15a)-Fe(10)-S(12) 124.5(2).

practically identical to those shown in Figure 2. Two $MoFe_3S_4$ cubanes are linked through symmetry-related S(12)-Fe(10/10a)-S(12a) bridges that generate an interior Fe_2S_2 rhomb in which Fe(10,10a) are additionally bridged to the cubanes over two μ_3-S atoms. Tetrahedral coordination at these atoms is severely distorted by two S-Fe-S angles near 125°. In the $Mo_2Fe_8S_{12}$ fragment, the cubane units do not share a common atom, but S(12) performs a μ_5 function by bridging within the cubane and the central rhomb. A relationship does exist between the central and terminal fragments in that μ_5-S(12) may be related to μ_6-S(9) and μ_3-S(14,15) to μ_2-S(7)/μ_3-S(8). Possibly one fragment is an intermediate in the formation of the other. Note that $Mo_2Fe_8S_{12}$ can be formally recovered from $Mo_2Fe_6S_9$ by insertion of Fe(10,10a) and S(12a,14a,15a) and attendant structural rearrangement.

The zero-field Moessbauer spectrum of polycrystalline complex **4** at 150 K in Figure 4A consists of a doublet (δ = 0.47 mm s^{-1}, quadrupole splitting ΔE_Q = 0.8 mm s^{-1}) and a (non-Lorentzian) linewidth of 0.45 mm s^{-1}. The broad lines suggest that ΔE_Q values of the six inequivalent iron sites differ somewhat and occur in the range of 0.75–1.1 mm s^{-1}. The lines in the spectrum at 4.2 K are even broader and have broad wings reminiscent of paramagnetic relaxation. To determine whether **4** is diamagnetic or paramagnetic, the cluster has been studied in applied fields up to 8.0 T. The

  1433-7851/99/3813-2068 $ 17.50+.50/0

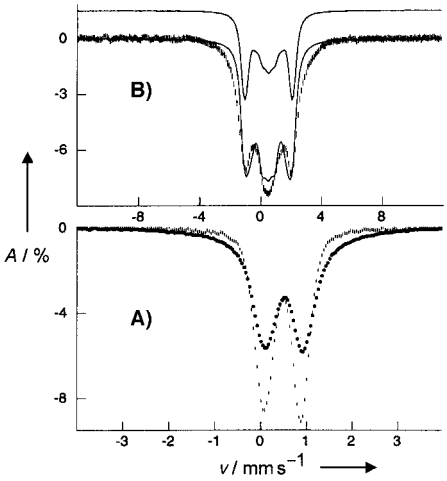

Figure 4. Moessbauer spectra of polycrystalline complex **4**. A) Spectra in zero field at 150 K (hash marks) and 4.2 K (solid circles). B) Spectrum at 4.2 K in a parallel applied field of 8.0 T. The solid line above the data is a simulation assuming that all iron sites reside in diamagnetic environments. The solid line drawn through the data is a simulation assuming one site with $\Delta E_Q = 0.8$ mm s^{-1}, $\delta = 0.52$ mm s^{-1}, and $\eta = 1$ (see text). The simulation assumes that the compound is paramagnetic with the undetermined ground-state spin S and involves zero-field splitting parameters and an A tensor chosen such that $H_{int}(x) = -4$ T and $H_{int}(y) \approx H_{int}(z) \approx 0$. The simulated spectrum is meant to illustrate how the shape of the high-field spectrum may arise.

spectrum in Figure 4B has a rather odd shape. While the splitting conforms to that of a diamagnet, there is additional intensity in the middle of the spectrum which cannot be explained by assuming, for instance, inequivalent iron sites. The increased intensity in the center of the spectrum at 8.0 T, however, can be understood as follows: If the asymmetry parameter of the electric field gradient tensor, $\eta = (V_{xx} - V_{yy})/V_{zz}$, has the value 1.0, the component of the field gradient along x is zero. If there is a negative *internal* magnetic field of $H_{int} = -4$ T along x, the effective field $H_{eff} = H_{int} + H_{applied}$ will be $H_{eff} = +4$ T. Because there is no quadrupole splitting along x, the x direction contributes a single line in the center of the spectrum that is broadened by the action of H_{eff}. The solid line through the data (Figure 4B) was obtained by assuming one iron site with $\eta = 1$ and $H_{int}(x) = -4.0$ T. The spectra of **4** exhibit magnetic features at 4.2 K, but it is not clear whether the system of 20 iron sites should be considered as an isolated paramagnet with unknown ground state spin or whether incipient long range magnetism gives rise to the internal magnetic field observed at 4.2 K.

We have demonstrated that reaction of **3** with HS^- induces substantial structural rearrangement to afford **4**, whose fragments can be related to different stages of the reaction. Taking the isomer shifts of Fe^{III}–rubredoxin (0.25 mm s^{-1}) and Fe^{II}–rubredoxin (0.70 mm s^{-1}) as criteria, the iron sites of **4** ($\delta =$ 0.52 mm s^{-1} at 4.2 K) have an oxidation state of +2.4.[17] The $Mo_2Fe_6S_9$ fragment provides the closest synthetic approach thus far to the topology of the P-cluster **1**. The Moessbauer spectrum of the P^N state shows sites with $\Delta E_Q \approx 3.0$ mm s^{-1} (two sites), 1.3 mm s^{-1} (one site), and 0.9 mm s^{-1} (five sites). Cluster **4** exhibits the sites with small ΔE_Q values characteristic of the P-cluster, but not the sites corresponding to the large ΔE_Q values. Lastly, we associate the formation of higher nuclearity Fe–S and Mo-Fe-S clusters (Fe_nS_n, $n = 8$, 16;[12b] **3**,[11] **4**) with their dominant Fe^{II} character.

Experimental Section

All operations were carried out under a pure dinitrogen atmosphere; solvent was removed in vacuo at room temperature. NMF (Aldrich) was stored over $NaHCO_3$ and distilled in vacuo. A solution of $(Et_4N)(SH)$ (99 mg, 0.61 mmol; Aldrich, recrystallized from acetonitrile/diethyl ether) in acetonitrile (20 mL) was added with stirring onto solid $[(Cl_4cat)_2Mo_2Fe_6S_8(PEt_3)_6]$ (600 mg, 0.30 mmol).[11] The brown suspension was stirred overnight, causing most of the solid to dissolve. The mixture was taken to dryness to remove H_2S and PEt_3. The solid residue was dissolved in acetonitrile (10 mL), the solution was stirred for 2 h, and the solvent was evaporated. The black residue was extracted with acetonitrile (20 mL). The extract was filtered through Celite, and $(Bu_4N)(PF_6)$ (80 mg, 0.21 mmol) was added to the filtrate, which was then reduced to dryness. The black residue was extracted with a minimal volume (4 mL) of NMF/diethyl ether (1/1 v/v). Vapor diffusion of diethyl ether into the extract over 3 d resulted in the separation of a highly crystalline solid, which was collected, washed with NMF/diethyl ether (1/1 v/v) and diethyl ether, and dried in vacuo. The product was obtained as 200 mg (33 % based on Fe) of an air-sensitive black crystalline solid, $(Bu_4N)_2(Et_4N)_6[(Cl_4cat)_6(PEt_3)_6Mo_6Fe_{20}S_{30}] \cdot 9$ NMF. UV/Vis (acetonitrile): λ_{max} (ε_M) = 224 (350000), 316 (146000), 450 nm (111000 M^{-1}cm^{-1}); cyclic voltammetry (acetonitrile, 20 mV s^{-1}, V vs. SCE): −0.45, −0.78 (oxidation), −1.01, −1.35, −1.56, −1.69 (reduction). Isomer shifts of ^{57}Fe are relative to that of iron metal at 298 K.

Diffraction-quality crystals were grown by diffusion of diethyl ether into the NMF extract obtained as described above. Crystal data for $(Bu_4N)_2(Et_4N)_6$[**4**]$\cdot 9$ NMF: $C_{170}H_{327}Cl_{24}Fe_{20}Mo_6N_{17}O_{21}P_6S_{30}$, $M_r = 6636.55$ g mol^{-1}, monoclinic, space group $P2_1/c$, $a = 19.3022(3)$, $b = 18.3633(1)$, $c = 36.9683(4)$ Å, $\beta = 91.501(1)^\circ$, $V = 13099.0(3)$ Å^3, $Z = 2$. Data were collected on a Siemens SMART diffractometer ($Mo_{K\alpha}$, 153 K). Of the 59074 reflections measured, 22676 were employed in structure solution and refinement. An empirical absorption correction was applied (SADABS). The structure was solved by direct methods and difference Fourier maps, and was refined by a full-matrix least-squares treatment on F^2. All non-hydrogen atoms were described anisotropically except for those of disordered solvate molecules and cations. Hydrogen atoms at calculated positions with thermal parameters 1.2 × those of bonded carbon atoms were included in the final refinement. Because of disorder, some cation and solvate molecule atoms were refined on split positions. At convergence, $R_1 = 0.0868$, $wR_2 = 0.1956$, and GOF = 1.099. Crystallographic data (excluding structure factors) for the structure reported in this paper have been deposited with the Cambridge Crystallographic Data Centre as supplementary publication no. CCDC-116378. Copies of the data can be obtained free of charge on application to CCDC, 12 Union Road, Cambridge CB2 1EZ, UK (fax: (+44) 1223-336-033; e-mail: deposit@ccdc.cam.ac.uk).

Received: March 3, 1999 [Z13103IE]
German version: *Angew. Chem.* **1999**, *111*, 2199–2203

Keywords: cluster compounds · iron · molybdenum · nitrogenases · Moessbauer spectroscopy

[1] H. Beinert, R. H. Holm, E. Münck, *Science* **1997**, *277*, 653–659.
[2] R. H. Holm, *Pure Appl. Chem.* **1995**, *67*, 217–224.
[3] J. B. Howard, D. C. Rees, *Chem. Rev.* **1996**, *96*, 2965–2982.
[4] J. W. Peters, M. H. B. Stowell, S. M. Soltis, M. G. Finnegan, M. K. Johnson, D. C. Rees, *Biochemistry* **1997**, *36*, 1181–1187.
[5] B. K. Burgess, D. J. Lowe, *Chem. Rev.* **1996**, *96*, 2983–3011.
[6] a) J. Huang, S. Mukerjee, B. M. Segal, H. Akashi, J. Zhou, R. H. Holm, *J. Am. Chem. Soc.* **1997**, *119*, 8662–8674; b) J. Huang R. H. Holm, *Inorg. Chem.* **1998**, *37*, 2247–2254.
[7] B. H. Huynh, E. Münck, W. H. Orme-Johnson, *Biochim. Biophys. Acta* **1979**, *527*, 192–203.

  1433-7851/99/3813-2069 $ 17.50+.50/0

[8] F. M. MacDonnell, K. Ruhlandt-Senge, J. J. Ellison, R. H. Holm, P. P. Power, *Inorg. Chem.* **1995**, *34*, 1815 – 1822.
[9] H.-I. Lee, B. J. Hales, B. M. Hoffman, *J. Am. Chem. Soc.* **1997**, *117*, 11 395 – 11 400.
[10] P. A. McLean, V. Papefthymiou, W. H. Orme-Johnson, E. Münck, *J. Biol. Chem.* **1987**, *262*, 12 900 – 12 903.
[11] K. D. Demadis, C. F. Campana, D. Coucouvanis, *J. Am. Chem. Soc.* **1995**, *117*, 7832 – 7833. The compound was reported in monoclinic space group $P2_1/c$. Upon recrystallization from dichloromethane/acetonitrile, we obtained the compound (unsolvated) in triclinic space group $P\bar{1}$ with $a = 13.549(3)$, $b = 14.114(3)$, $c = 23.654(5)$ Å, $\alpha = 76.04(3)$, $\beta = 86.02$, $\gamma = 62.57°$, $V = 3892(1)$ Å^3, and $Z = 2$. The refined structure is essentially identical to that reported. Cl_4cat = tetrachlorocatecholate(2 –).
[12] a) M. A. Tyson, K. D. Demadis, D. Coucouvanis, *Inorg. Chem.* **1995**, *95*, 4519 – 4520; b) C. Goh, B. M. Segal, J. Huang, J. R. Long, R. H. Holm, *J. Am. Chem. Soc.* **1996**, *117*, 11 844 – 11 853.
[13] J.-F. You, G. C Papaethymiou, R. H. Holm, *J. Am. Chem. Soc.* **1992**, *114*, 2697 – 2710.
[14] T. Krüger, B. Krebs, G. Henkel, *Angew. Chem.* **1989**, *101*, 54 – 55; *Angew. Chem. Int. Ed. Engl.* **1989**, *28*, 61 – 62.
[15] K. B. Musgrave, H. I. Liu, L. Ma, B. K. Burgess, G. Watt, B. Hedman, K. O. Hodgson, *J. Biol. Inorg. Chem.* **1998**, *3*, 344 – 352.
[16] a) E. Nordlander, S. C. Lee, W. Cen, Z. Y. Wu, C. R. Natoli, A. Di Cicco, A. Filipponi, B. Hedman, K. O Hodgson, R. H. Holm, *J. Am. Chem. Soc.* **1993**, *115*, 5549 – 5558; b) W. Cen, F. M. MacDonnell, M. J. Scott, R. H. Holm, *Inorg. Chem.* **1994**, *33*, 5809 – 5818.
[17] The isomer shift is essentially the same as that for an individual $[MoFe_3S_4]^{2+}$ cluster ($\delta \approx 0.54$ mm s^{-1} at 4.2 K): P. K. Mascharak, G. C. Papaefthymiou, W. H. Armstrong, S. Foner, R. B. Frankel, R. H. Holm, *Inorg. Chem.* **1983**, *22*, 2851 – 2858. The value is less than 0.7 mm s^{-1}, presumably because of electron delocalization into the molybdenum site.

Deposition of Data from X-Ray Structure Analyses

In order to make life easier for authors and referees the Cambridge Crystallographic Data Centre (CCDC) and the Fachinformationszentrum Karlsruhe (FIZ) have unified their procedures for the depostion of data from single-crystal X-ray structure analyses.

Prior to submitting a manuscript please deposit the data for your compound(s) **electronically** at the appropriate date base, that is, at the CCDC for organic and organometallic compounds and at the FIZ for inorganic compounds. Both data bases will be pleased to provide help (see our *Notice to Authors* in the first issue of this year). In general, you will receive a depository number from the data base within two working days after electronic deposition; please include this number with the appropriate standard text (see our Notice to Authors) in your manuscript. This will enable the referees to retrieve the structure data quickly and efficiently if they need this information to reach their decision.

This is now the uniform procedure for manuscripts submitted to the journals *Advanced Materials, Angewandte Chemie, Chemistry–A European Journal, the European Journal of Inorganic Chemistry, and the European Journal of Organic Chemistry.*

  1433-7851/99/3813-2070 $ 17.50+.50/0